Multi-decadal record of ice dynamics on Daugaard Jensen Gletscher, East Greenland, from satellite imagery and terrestrial measurements

Leigh A. STEARNS,[1] Gordon S. HAMILTON,[1] Niels REEH[2]

[1]*Climate Change Institute, and Department of Earth Sciences, University of Maine, 303 Bryand Global Sciences Center, Orono, ME 04469-5790, USA*
E-mail: leigh.stearns@maine.edu
[2]*Department of Electromagnetic Systems, Technical University of Denmark, DK-2800 Kgs. Lyngby, Denmark*

ABSTRACT. The history of ice velocity and calving front position of Daugaard Jensen Gletscher, a large outlet glacier in East Greenland, is reconstructed from field measurements, aerial photography and satellite imagery for the period 1950–2001. The calving terminus of the glacier has remained in approximately the same position over the past ~50 years. There is no evidence of a change in ice motion between 1968 and 2001, based on a comparison of velocities derived from terrestrial surveying and feature tracking using sequential satellite images. Estimates of flux near the entrance to the fjord vs snow accumulation in the interior catchment show that Daugaard Jensen Gletscher has a small negative mass balance. This result is consistent with other mass-balance estimates for the inland region of the glacier.

INTRODUCTION

A recent program to study the mass balance of the Greenland ice sheet demonstrated that the largest changes are currently taking place near the ice-sheet margins (Thomas and others, 2001). Thinning rates of several meters per year were observed on large outlet glaciers draining the southeast portion of the ice sheet (Krabill and others, 2001), and grounding line retreats of several kilometers were measured on glaciers in North Greenland (Rignot and others, 2001). The calving front of Jakobshavn Isbræ, Greenland's largest glacier, recently retreated ~5 km (based on examination of satellite imagery acquired in 2003) after occupying a quasi-stable position for the previous ~30 years (Sohn and others, 1998). Conversely, extensive regions of the high-elevation ice-sheet interior appear to be close to steady-state conditions (Thomas and others, 2000). Current research is directed towards explaining the distribution of these observed changes.

Abdalati and others (2001) suggested that the rapid thinning rates observed in southeast Greenland were initiated as recently as the early 1990s. Air temperatures measured at coastal stations show a cooling trend for most of the 20th century (Box, 2002), but temperatures have been warming since the 1980s. However, glacier thinning rates are too large to be explained by variability in climate (air temperature, snowfall) alone. An alternative explanation is that the observed thinning is a response to changes in ice dynamics, such as an increase in ice velocities. One mechanism that might account for faster ice motion is an increase in the amount of basal lubrication, perhaps as a result of enhanced surface melting (e.g. Zwally and others, 2002). Unfortunately, very few glaciers in Greenland have the long records of ice velocities that are necessary to test this hypothesis.

In this paper, we report the results of a study on Daugaard Jensen Gletscher, one of the largest and fastest-flowing outlet glaciers in East Greenland (Fig. 1). We base our analysis on a combination of field measurements conducted in the 1960s, mapping of flow velocities from modern high-resolution Advanced Spaceborne Thermal Emission and Reflection Radiometer (ASTER) satellite imagery, and an examination of calving front positions from archival image sources acquired since the 1950s. The data are used to test for recent changes in ice-flow regime, and to compare ice dynamics with mass-balance conditions for the glacier.

Daugaard Jensen Gletscher terminates in tidewater at the head of Nordvestfjord, the northernmost branch of the Scoresby Sund fjord system (Fig. 1). Two smaller outlet glaciers from the same catchment basin, Charcot Gletscher and Graah Gletscher (called F. Graae Gletscher on some maps), also terminate at tidewater in tributary fjords. The main glacier drains about 4% of the ice sheet and reaches sustained speeds of about 4 km a^{-1} near its grounding line (Reeh and Olesen, 1986). Mass-balance estimates for the upstream region of the inland ice sheet indicate a small negative balance to steady-state conditions (Thomas and others, 2000; Krabill and others, 2001; Hamilton and Whillans, 2002). The availability of ice velocity measurements from 1968 and 2001 makes Daugaard Jensen Gletscher a useful location to test for recent changes in ice dynamics, and to examine the effects of ice flow on the ice-sheet interior.

The analysis shows that the flow of Daugaard Jensen Gletscher apparently did not change between 1968 and 2001. Between 1950 and 2001, the calving front occupied a nearly constant position in the fjord. These results are largely consistent with the mass-balance conditions observed on the inland ice sheet. An implication of this work is that the conditions forcing a hypothesized change in ice dynamics in southeast Greenland are not yet operating this far north.

CALVING FRONT POSITIONS, 1950–2001

The lower 28 km long trunk of Daugaard Jensen Gletscher is constrained in a 5–7 km wide fjord. The glacier appears to be floating within about 4 km of the calving front, based on the change in crevasse patterns observed in satellite imagery. The inferred grounding line position is taken as the point
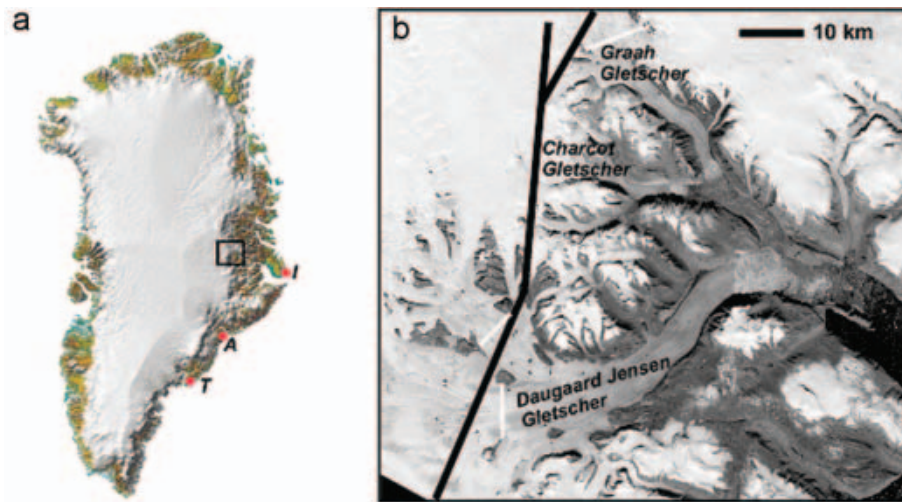
Fig. 1. (a) Map of the study area and nearby automatic weather stations, from Box (2002). The weather stations are marked with circles and referred to in the text as Illoqqortoormiut (I), Aputiteeq (A) and Tasiilaq (T). (b) Landsat-7 scene showing the location of studied glaciers in northwestern Scoresby Sund, East Greenland. Thick black lines show the locations of the airborne radar profiles (Gogineni and others, 2001). Thin white lines show the location of mass-balance flux gates.

where crevasses become noticeably wider. Ice thickness at the calving margin is ~500 m, from the dimensions of capsized icebergs in the fjord immediately in front of the glacier (Dowdeswell and others, 1992), and from hydrostatic equilibrium based on a measured terminus freeboard height of ~60 m (Reeh and Olesen, 1986).

Charcot and Graah glaciers are constrained in ~2 km wide fjords, 12 and 26 km long, respectively. Ice thicknesses for both glaciers are smaller than for Daugaard Jensen Gletscher. Measurements of terminus freeboard heights yield thicknesses of ~240 m for Charcot Gletscher and ~320 m for Graah Gletscher (Olesen and Reeh, 1969).

A record of calving front positions is reconstructed for each glacier using modern and archival imagery, and survey data. The earliest observations are oblique aerial photographs taken in 1950 (Weidick, 1995). Survey measurements were made at the terminus of each glacier in 1968 (Reeh and Olesen, 1986). Additional observations were made using Landsat 3 (1973), Landsat 5 (1991) and Landsat 7 imagery (1999). The most recent calving front positions were mapped using ASTER imagery acquired in 2001.

The calving front position of Daugaard Jensen Gletscher has remained remarkably constant throughout the 51 years of observation (Fig. 2). Small variations in position are probably the result of annual or seasonal fluctuations in the rate of iceberg production (Olesen and Reeh, 1969). The widening and ~400 m deepening of the fjord a few kilometers in front of the calving margin (Ó Cofaigh and others, 2001) probably limits the forward extension of the glacier. The grounding line position, to the extent that the location of sudden crevasse widening can be mapped in the record, also appears to have been relatively stable (within ~250 m, based on the pixel resolution and geolocation uncertainties of archival imagery). This stability indicates that ice flux to the grounding line has remained constant, and might also be an indication that basal melt rates have not increased in recent decades (cf. Rignot and others, 2001).

The terminus position records for Charcot and Graah glaciers appear to indicate out-of-phase behavior of the neighboring glaciers. Olesen and Reeh (1969) note that Charcot Gletscher retreated ~2 km between 1933 and 1950,

and retreated another ~1 km between 1950 and 1968. During the same period, Graah Gletscher maintained a stable front position. The terminus of Charcot Gletscher remained at the same position between 1968 and 2001 (Fig. 2). Graah Gletscher retreated 1–2 km between 1991 and 1999 but changed very little in the last 2 years of observation (Fig. 2). It appears that both glaciers are in long-term retreat, although it is interesting to note that retreat events seem to occur episodically during longer stages of front position stability.

GLACIER VELOCITIES, 1968–2001

The flow pattern of Daugaard Jensen Gletscher was first measured in the late 1960s by Olesen and Reeh (1969) using terrestrial surveying techniques. Velocities were obtained by repeated theodolite intersections from bedrock stations to natural targets on the glacier surface. Most of the targets were located on the floating portion of the glacier, although some points were measured just upstream of the grounding line. The measurements were made over a period of 32 days, and the velocities expressed as annual averages. Reeh and Olesen (1986) noted velocity fluctuations of up to 2 m d^{-1}, or 15% of total motion, at the front of the glacier. The possibility of these fluctuations being forced by fjord tides, as observed on Jakobshavn Isbræ (Echelmeyer and Harrison, 1990), was not supported by the duration and amplitude of the oscillations (Reeh and Olesen, 1986). Insead, these velocity fluctuations imply lubrication at the base of Daugaard Jensen Gletscher. The presence of basal meltwater from Daugaard Jensen Gletscher is also evident from a nearby sediment core. The sediment core, drilled 5 km down-fjord from the calving front of Daugaard Jensen Gletscher, consisted of well-defined, laminated muds (Ó Cofaigh and others, 2001). Laminated muds suggest an abundance of meltwater being delivered into the fjord. Isotopically light water, sampled at the core site, supports this interpretation (Ó Cofaigh and others, 2001).

The modern flow pattern of the glacier was obtained by applying a feature-tracking technique (Scambos and others, 1992) to sequential satellite images acquired by the ASTER sensor in August 2000 and July 2001. High-resolution (15 m

pixel size) visible band data were used. The displacement of surface features (crevasses, seracs) was derived by matching patterns of brightness in a reference chip from the first image to identical patterns in a search box from the second image using an automatic cross-correlation technique.

Before implementing the matching routine, the two images were geocoded using satellite ephemeris data and co-registered using manual tie points. A principal component filter was applied to both scenes to reduce image noise. Scambos and others (1992) noted that the use of Landsat imagery required additional noise suppression techniques, namely scan-line de-striping, high-pass filtering and Gaussian contrast stretching, but these steps were not necessary for preparing the ASTER images. The feature tracking was performed with a reference chip of 4×4 pixels and a search box of 128×32 pixels. The location of the search box and its long axis orientation were based on a priori estimates of the glacier flow field.

The selection of the image pair was based on several considerations. Both images were required to be largely cloud-free and have similar illumination characteristics. The ASTER instrument has the capability for across-track off-nadir scene acquisition ($-24°$ to $+24°$ from nadir). This capability unfortunately limits the number of potential matching pairs, because different scene acquisition geometries lead to different image illumination characteristics. Stearns and Hamilton (2005) note that, for regions of rugged terrain such as coastal East Greenland, pointing angles of sequential images need to be within $3°$ to maintain common illumination characteristics. An additional consideration was the length of time between scene acquisition dates. The time interval had to be long enough to allow detectable feature displacement, but not too long such that features were distorted beyond recognition. Based on these criteria, two scenes acquired in August 2000 and July 2001 were selected for feature tracking.

Uncertainties in derived velocities are dominated by errors in image co-registration and the application of the cross-correlation technique. The presence of static features (mountain peaks, rock ridges) was used to minimize image-to-image registration errors to ~1 pixel. Uncertainties associated with the cross-correlation technique were quantified by examining the apparent displacement of static features in the images. These displacements never exceeded 1 pixel (15 m). Any matches over the glacier surface with residuals larger than 1 pixel were therefore discarded. Cumulatively, the uncertainties resulting from all error sources ($\sim 50\,\mathrm{m\,a^{-1}}$) are unimportant for the fast glacier speeds ($>1000\,\mathrm{m\,a^{-1}}$) being investigated in the current study.

The feature-tracking technique yielded displacement vectors over most of the length of Daugaard Jensen Gletscher, from where it enters the fjord to the grounding line (Fig. 3). Velocity vectors were also obtained for most of Graah Gletscher (Fig. 4) using the same image pair. On the floating part of Daugaard Jensen Gletscher, within ~4 km of the calving front, large longitudinal extension rates caused crevasses to be deformed beyond recognition from one image to the next (~1 year interval). A shorter interval between images might have produced trackable features for velocity mapping in this portion of the glacier, but no suitable images were available.

The results show that the speed of Daugaard Jensen Gletscher steadily increases with distance along the fjord (Fig. 3). Peak speeds near the grounding line are $\sim 3\,\mathrm{km\,a^{-1}}$.
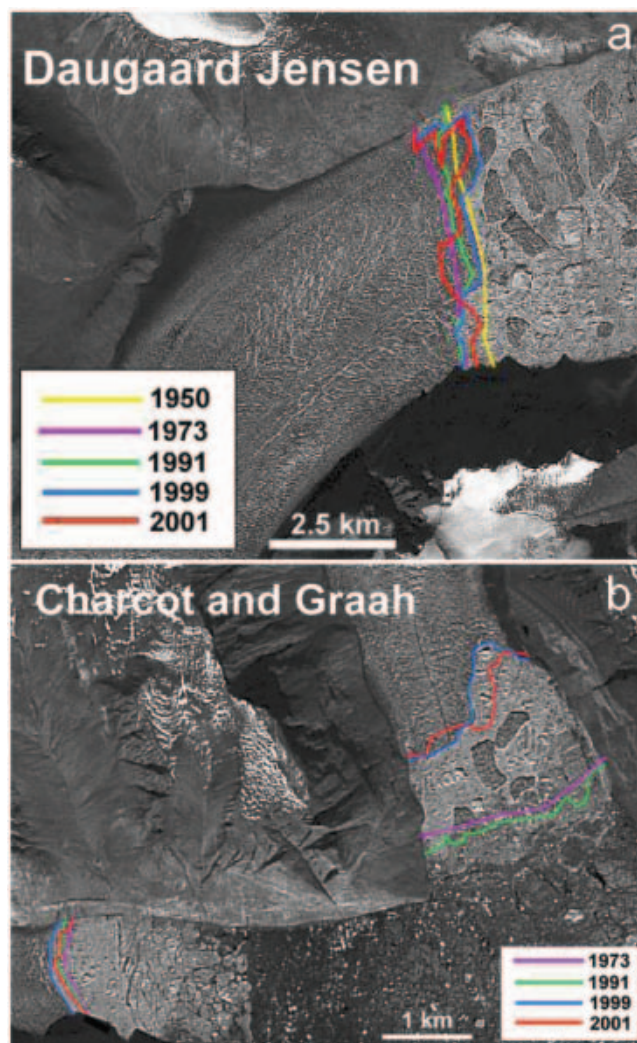
Fig. 2. Terminus positions for Daugaard Jensen Gletscher (a), Charcot Gletscher (b, left) and Graah Gletscher (b, top). Positions were obtained from aerial photography in 1950 (photograph #11947 in Weidick, 1995); in 1973 by Landsat 3 (scene #124009007320790); in 1991 by Landsat 5 (scene #P231R09_5T19910621); in 1999 by Landsat 7 (scene #P231R009_7FL19990705); and in 2001 by ASTER (scene #003_07122001140515_11172003002110).

Reeh and Olesen (1986) reported faster speeds of $\sim 4\,\mathrm{km\,a^{-1}}$ near the front of the floating terminus. Graah Gletscher reaches sustained speeds of $\sim 1\,\mathrm{km\,a^{-1}}$ in its lower reaches. The longitudinal profile of velocity for Graah Gletscher seems to indicate a rapid jump in speed as ice enters the fjord (Fig. 4). Velocities increase steadily with distance down the glacier, but peak speeds do not reach those of Daugaard Jensen Gletscher, as would be expected from the shallower ice thicknesses.

A comparison of ice velocities from 1968 and 2001–02 is possible for the region just inland of the grounding line on Daugaard Jensen Gletscher where terrestrial and satellite measurements overlap. At this location (7.5 km from the calving terminus), Reeh and Olesen (1986) report an average annual velocity of $2.70 \pm 0.15\,\mathrm{km\,a^{-1}}$. The velocity derived from satellite imagery is $2.65 \pm 0.05\,\mathrm{km\,a^{-1}}$. Both results are consistent, given the uncertainties associated with each technique. The comparison shows that the annually averaged speed of the glacier was not substantially different in 1968 and 2001.
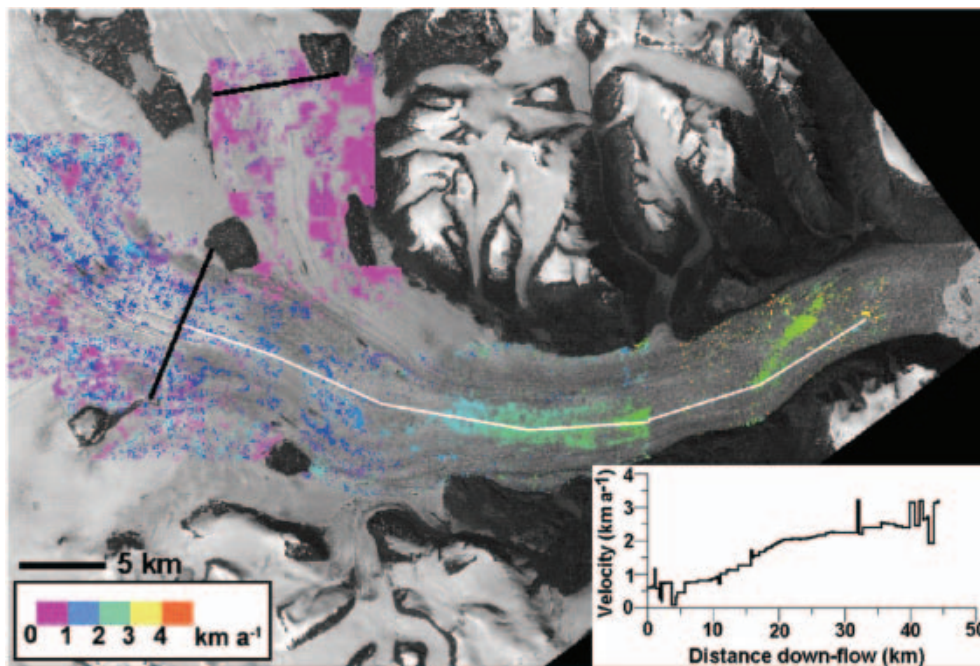
Fig. 3. Ice velocities for Daugaard Jensen Gletscher obtained from feature tracking, overlaid on an ASTER image. Black lines represent mass-balance flux gates. The white box shows the region with overlapping velocity measurements from 1968. Inset shows a velocity profile along the thin white line.

No direct comparison is possible for Graah Gletscher. Olesen and Reeh (1969) obtained velocities for the calving front from surveys conducted 6 days apart in the summer of 1968. Converted to an annual average, velocities across the terminus were $1.5 \pm 0.15 \, \text{km a}^{-1}$. No displacement vectors for the terminus were obtained using the feature-tracking technique on satellite images, probably because crevasse shapes changed beyond recognition from one image to the next. The velocities obtained closest to the calving front ($\sim$4 km up-glacier) during 2000–01 were approximately $0.95 \pm 0.05 \, \text{km a}^{-1}$ and appeared to be increasing towards the terminus (Fig. 4).

ESTIMATING MASS BALANCE

The velocity measurements can be combined with accumulation rate maps to estimate the mass balance (F_{net}) of the Daugaard Jensen Gletscher catchment. Dimensions of the catchment basin (SA) were obtained from a high-resolution elevation model of the ice sheet (Bamber and others, 2001). There are several estimates for snow accumulation rate (b) within the catchment, based on interpolation between numerous isolated ice-core records (e.g. Bales and others, 2001; Zwally and others, 2001). The mean of these estimates is used to obtain mass added to the catchment (F_{in}). Ideally, outgoing flux (F_{out}) should be obtained at the grounding line. However, feature tracking using satellite images failed to produce velocities on this part of the glacier, so alternative flux gates were chosen close to the locations of airborne ice-penetrating radar profiles (Gogineni and others, 2001) (Fig. 1). Two gates were selected to cover the main tributaries converging at the head of the fjord. Each gate was rotated slightly from the flight-line so as to be orthogonal to the measured ice-flow vectors.

Similar procedures were followed for Graah Gletscher, except for the location of the flux gate. The radar flight-lines cross the glacier up-flow of the available satellite image-derived velocities. In order to use the measured velocities, the geometry of a flux gate coinciding with satellite coverage was obtained from an ice-thickness compilation of Bamber and others (2001).

Comparing catchment-wide snow accumulation rates with ice fluxes through Daugaard Jensen and Graah glaciers reveals a small negative mass balance equivalent to an average thinning rate of $-8.24 \pm 5.51 \, \text{cm a}^{-1}$ (Table 1). This
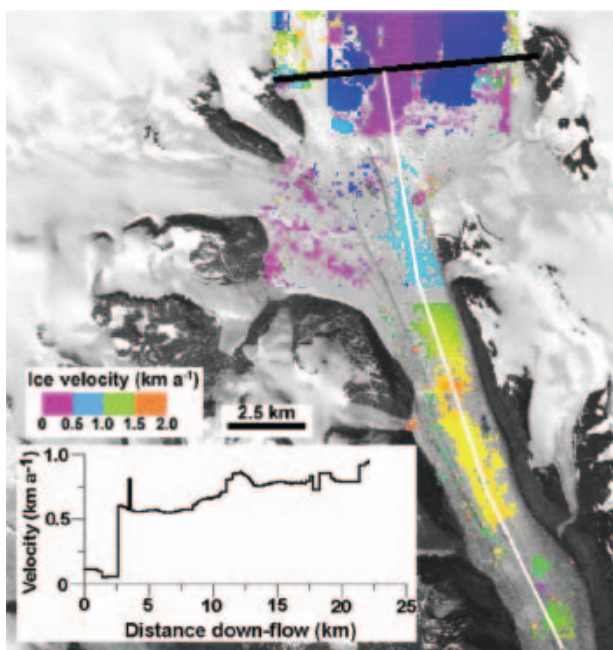
Fig. 4. Ice velocities for Graah Gletscher obtained from feature tracking, overlaid on an ASTER image. Inset shows a velocity profile along the thin white line.

Table 1. Quantities used to estimate mass balance

Catchment, SA	$50\,030 \pm 500\,\text{km}^2$
Accumulation, b	$0.245 \pm 0.07\,\text{m a}^{-1}$
Flux in, F_{in}	$11.4 \pm 2.6\,\text{km}^3\,\text{a}^{-1}$
Flux out, F_{out}	$15.2 \pm 0.3\,\text{km}^3\,\text{a}^{-1}$
Mass balance, F_{net}	$-3.8 \pm 2.5\,\text{km}^3\,\text{a}^{-1}$

value is smaller than a local thinning rate of $-28.1 \pm 20.4\,\text{cm a}^{-1}$ obtained by Hamilton and Whillans (2002) at a site 100 km up-glacier in the catchment area. However, considering the respective uncertainties, both results are statistically similar.

A similar analysis was performed by Rignot and others (2004) using flow velocities obtained by interferometric processing of radar images from 1996 and a slightly different catchment accumulation rate. Their results are consistent with the present analysis, given the uncertainties in each technique.

DISCUSSION

Our results of near-steady-state conditions in the Daugaard Jensen Gletscher catchment are quite different from the large thinning rates (several meters per year) observed 500–700 km farther south in Greenland (e.g. Kangerdlugssuaq Gletscher) (Abdalati and others, 2001). The factors driving rapid thinning of these glaciers do not appear to be acting at the current time in the northwestern Scoresby Sund region. One hypothesis is that increased surface melt reaching the bed has caused these southeastern glaciers to accelerate and thin (Abdalati and others, 2001; Krabill and others, 2001). This explanation is supported by satellite passive microwave emissivity data revealing a 16% increase in southeast Greenland melt area from 1979 to 2002 (Abdalati and Steffen, 2001). While the spatial extent of surface melting fluctuates annually due to weather patterns and volcanic eruptions, there is a consistently larger melt extent in southeastern Greenland (near Kangerdlugssuaq and other rapidly thinning glaciers) than in central East Greenland inland of Scoresby Sund.

Coastal temperature records are consistent with the passive microwave data. From 1961 to 1990, the annual mean temperatures at Aputiteeq and Tasiilaq, the weather stations closest to Kangerdlugssuaq Gletscher and other thinning glaciers in the southeast, were ~6°C warmer than at Illoqqortoormiut near the mouth of the Scoresby Sund fjord system (Box, 2002). A 1°C warming for 1985–2000, with continued warming since 2001, was also recorded at the southeast stations (Box, 2002), implying a greater availability of meltwater for basal lubrication of glaciers in that region.

No clear warming trend was observed at Illoqqortoormiut over the last few decades (Box, 2002), suggesting that meltwater production on glaciers in the region has not increased. It is important to note that Daugaard Jensen Gletscher is located ~300 km from the weather station, and that it is likely that the inner part of the Scoresby Sund fjord system experiences cooler continental conditions. However, the climate record at Illoqqortoormiut is consistent with the stable ice dynamics of Daugaard Jensen Gletscher between 1968 and 2001.

CONCLUSIONS

An analysis of remote-sensing observations and field measurements indicates near-steady-state conditions for the last ~50 years in the Daugaard Jensen Gletscher region of central East Greenland. Ice velocities near the terminus, obtained from terrestrial theodolite surveys in 1968, are similar to those obtained at the same location by tracking surface features in satellite images from 2000 and 2001. The calving front of Daugaard Jensen Gletscher remained in approximately the same position throughout the period of observation 1950–2001. This result is consistent with the constant flux of ice to the grounding line, indicated by the steady velocities. It also suggests that there has been no increase in basal melting beneath the floating section of the glacier tongue, in contrast to observations elsewhere in Greenland (Rignot and others, 2001). The terminus positions of Charcot and Graah glaciers, two smaller glaciers in the same system, show long-term retreat, although most of the retreat occurs episodically between longer phases of stable front positions.

The mass budget of the glacier catchment, estimated using measured velocities, accumulation rates and surface and bed topographies, indicates a very small negative balance. This result is consistent with slow thinning rates calculated for sites inland of the fjord (Krabill and others, 2001; Hamilton and Whillans, 2002). The currently stable ice dynamics of the outlet glacier trunk do not appear to be the cause of this small negative balance, although it is not possible to ascertain if glacier speeds increased during an earlier period of warming in the first half of the 20th century (Box, 2002).

REFERENCES

Abdalati, W. and K. Steffen. 2001. Greenland ice sheet melt extent: 1979–1999. *J. Geophys. Res.,* **106**(D24), 33,983–33,988.

Abdalati, W. *and 8 others.* 2001. Outlet glacier and margin elevation changes: near-coastal thinning of the Greenland ice sheet. *J. Geophys. Res.,* **106**(D24), 33,729–33,742.

Bales, R.C., J.R. McConnell, E. Mosley-Thompson and B. Csatho. 2001. Accumulation over the Greenland ice sheet from historical and recent records. *J. Geophys. Res.,* **106**(D24), 33,813–33,825.

Bamber, J.L., S. Ekholm and W.B. Krabill. 2001. A new, high-resolution digital elevation model of Greenland fully validated with airborne laser altimeter data. *J. Geophys. Res.,* **106**(B4), 6733–6746.

Box, J.E. 2002. Survey of Greenland instrumental temperature records: 1873–2001. *Int. J. Climatol.,* **22**(15), 1829–1847.

Dowdeswell, J.A., R.J. Whittington and R. Hodgkins. 1992. The sizes, frequencies, and freeboards of East Greenland icebergs observed using ship radar and sextant. *J. Geophys. Res.,* **97**(C3), 3515–3528.

Echelmeyer, K. and W.D. Harrison. 1990. Jakobshavns Isbræ, West Greenland: seasonal variations in velocity – or lack thereof. *J. Glaciol.,* **36**(122), 82–88.

Gogineni, S. *and 9 others.* 2001. Coherent radar ice thickness measurements over the Greenland ice sheet. *J. Geophys. Res.,* **106**(D24), 33,761–33,772.

Hamilton, G.S. and I. Whillans. 2002. Local rates of ice-sheet thickness change in Greenland. *Ann. Glaciol.,* **35**, 79–83.

Krabill, W. *and 9 others*. 2001. Greenland Ice Sheet: high-elevation balance and peripheral thinning. *Science,* **289**(5478), 428–430.

Ó Cofaigh, C., J. Dowdeswell and H. Grobe. 2001. Holocene glacimarine sedimentation, inner Scoresby Sund, East Greenland: the influence of fast-flowing ice-sheet outlet glaciers. *Mar. Geol.,* **75**, 103–129.

Olesen, O.B. and N. Reeh. 1969. Preliminary report on glacier observations in Nordvestfjord, East Greenland. *Grønl. Geol. Undersøgelse Rapp.* 21, 41–53.

Reeh, N. and O.B. Olesen. 1986. Velocity measurements on Daugaard-Jensen Gletscher, Scoresby Sund, East Greenland. *Ann. Glaciol.,* **8**, 146–150.

Rignot, E., S. Gogineni, I. Joughin and W. Krabill. 2001. Contribution to the glaciology of northern Greenland from satellite radar interferometry. *J. Geophys. Res.,* **106**(D24), 34,007–34,019.

Rignot, E., D. Braaten, P. Gogineni, W.B. Krabill and J.R. McConnell. 2004. Rapid ice discharge from southeast Greenland glaciers. *Geophys. Res. Lett.,* **31**(10), L10401. (10.1029/2004GL019474.)

Scambos, T.A., M.J. Dutkiewicz, J.C. Wilson and R.A. Bindschadler. 1992. Application of image cross-correlation to the measurement of glacier velocity using satellite image data. *Remote Sens. Environ.,* **42**(3), 177–186.

Sohn, H.G., K.C. Jezek and C.J. van der Veen. 1998. Jakobshavn Glacier, West Greenland: thirty years of spaceborne observations. *Geophys. Res. Lett.,* **25**(14), 2699–2702.

Stearns, L.A. and G.S. Hamilton. 2005. A new velocity map for Byrd Glacier, East Antarctica from sequential ASTER satellite imagery. *Ann. Glaciol.,* **41**, 71–76.

Thomas, R. *and 6 others*. 2000. Mass balance of the Greenland ice sheet at high elevations. *Science,* **289**(5478), 426–428.

Thomas, R.H. and PARCA Investigators. 2001. Program for Arctic Regional Climate Assessment (PARCA): goals, key findings, and future directions. *J. Geophys. Res.,* **106**(D24), 33,691–33,705.

Weidick, A. 1995. Greenland. *In* Williams, R.S. and J.G. Ferrigno, eds. *Satellite image atlas of glaciers of the world. US Geol. Surv. Prof. Pap.* 1386-C.

Zwally, J.H. and M.B. Giovinetto. 2001. Balance mass flux and ice velocity across the equilibrium line in drainage systems of Greenland. *J. Geophys. Res.,* **106**(D24), 33,717–33,728.

Zwally, H.J., W. Abdalati, T. Herring, K. Larson, J. Saba and K. Steffen. 2002. Surface melt induced acceleration of Greenland Ice Sheet flow. *Science,* **297**, 218–222.